



## APPLYING FUZZY LOGIC CONTROLLER TO INTELLIGENT SOLAR PANEL CLEANING SYSTEM

Cong-Hui Huang

Department of Automation and Control Engineering, Far East University, Tainan County, Taiwan, R.O.C.,  
ch\_huang@cc.feu.edu.tw

Follow this and additional works at: <https://jmstt.ntou.edu.tw/journal>



Part of the [Controls and Control Theory Commons](#)

### Recommended Citation

Huang, Cong-Hui (2014) "APPLYING FUZZY LOGIC CONTROLLER TO INTELLIGENT SOLAR PANEL CLEANING SYSTEM," *Journal of Marine Science and Technology*. Vol. 22: Iss. 6, Article 8.

DOI: 10.6119/JMST-014-0321-8

Available at: <https://jmstt.ntou.edu.tw/journal/vol22/iss6/8>

This Research Article is brought to you for free and open access by Journal of Marine Science and Technology. It has been accepted for inclusion in Journal of Marine Science and Technology by an authorized editor of Journal of Marine Science and Technology.

---

## APPLYING FUZZY LOGIC CONTROLLER TO INTELLIGENT SOLAR PANEL CLEANING SYSTEM

### Acknowledgements

The author would like to thank the National Science Council of the Executive Yuan, Taiwan, R.O.C., for financially supporting this study under contract NSC 102-2221-E-269-016

# APPLYING FUZZY LOGIC CONTROLLER TO INTELLIGENT SOLAR PANEL CLEANING SYSTEM

Cong-Hui Huang

Key words: cleaning system, fuzzy logic controller, intelligent control, solar panel.

## ABSTRACT

This paper presents an intelligent solar panel cleaning system that utilizes a fuzzy logic controller. The output voltage of the solar panel is applied to calculate whether to activate the cleaning mechanism. The direction and position of the system is set using a light sensor that is parallel to the direction of the sunlight. The data from the light sensors, combined with fuzzy logic control software developed using LabVIEW, determine the control commands (stop, forward, and reverse) for the stepper motors controlling the cleaning process. The cleaning process, which is repeated until the power output from the solar panels is sufficient, is performed in real-time to maintain the power generating capacity of the solar cells. A water spray is activated in addition to the cleaning process, reducing the temperature of the solar cells and enabling maximal efficiency to be achieved.

## I. INTRODUCTION

The use of solar panels has extraordinary potential. In particular, Taiwan is favorably positioned geographically to benefit from high levels of sunlight. Solar panels have been widely applied in Taiwan, where many power-generating products operate in open air by using solar cells. However, because the solar panels are exposed to the elements, blemishes and deposits accumulate on the surfaces, reducing the efficiency of the output current. The dust particles create shadows on the solar cells, substantially reducing the energy conversion efficiency.

In addition, some dust particles are corrosive, reducing the life span of the solar cells and their supporting frames. The

elevated positioning of solar panels renders manual cleaning dangerous and inconvenient.

Using natural or renewable energy has been emphasized for sustainable energy generation. Renewable energy sources, including solar energy, wind power, hydropower, tidal power, ocean thermal energy conversion, and biomass, are all key topics for future research [1, 17]. In Taiwan, wind and solar power are the most viable renewable energy sources. However, wind power systems are suitable only in nonurban areas because the large amount of noise generated is impractical for residential areas.

The economic benefits and large scale of wind energy harvesting are a subject of contention [20]. Therefore, solar energy is more favorable for use in urban areas. The energy generated from the sun's rays over a 40-minute interval is equal to the total energy used in 1 year by the global population. Because Taiwan is located in a subtropical region relatively near the equator, sunshine is plentiful. Directly converting solar energy into electrical energy by using solar cells can afford clean energy; solar energy is pollution-free and noiseless. Thus, solar energy is a reasonable solution for sustainable development [18].

We propose using a fuzzy logic controller incorporated into a solar panel cleaning system. We applied fuzzy logic to determine the solar intensity based on the CdS circuit. Initially, under direct sunlight, the CdS value was 0.25 V, a level that indicated that the CdS has detected a light source. We then determined whether the energy conversion efficiency was too low for the solar panel. For example, if the output current of the solar panel is 0.1 A, and the test output value from the fuzzy program is 0.82756 (i.e., exceeding the 0.5 threshold), then the fuzzy program concludes that the output current has decreased to an insufficient level, and the cleaning process is activated. Similarly, if the detected CdS value is 0.25 V, and the output current of the solar panel is 0.95 A, then the test output value from the fuzzy program is 0.3195. This value (lower than 0.5) indicates that the output current is normal; therefore, cleaning is not activated. When the CdS value exceeds 0.140 V, the fuzzy program generates a value of zero, which indicates that no light source is detected (e.g., on overcast or rainy days and at dawn or dusk).

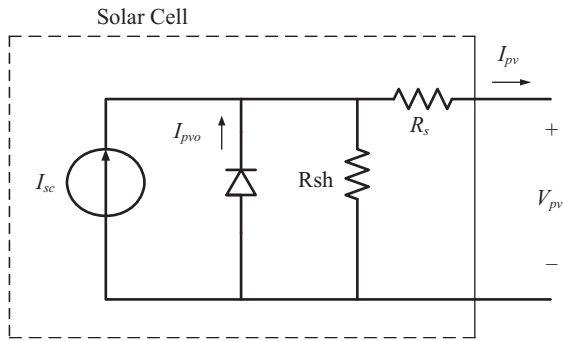


Fig. 1. Equivalent circuit of a solar cell.

## II. HARDWARE COMPONENT STRUCTURE

### 1. Solar Panel

A solar cell, also known as a photovoltaic cell (PV), uses a solar panel to absorb solar energy and convert it into direct current, which is then transformed into alternating or direct output current. Because the solar cell output voltage is typically extremely low, approximately 0.5-0.6 V, the cells are used in sets of 36 or 72 [9, 10]. Engineers often arrange the cells in various configurations to generate the voltage required. Therefore, producing solar energy requires substantial space.

Two main obstacles must be overcome before solar energy generation can be practical: space and efficiency. Once a solar panel is installed, the operation costs are identical to those of an electronic converter; thus, it is highly economical to operate. Two types of solar cells are widely used: bulk and thin-film cells [4, 5]. Bulk solar cells can be further classified into two subtypes: unisilicon and multisilicon cells. Unisilicon cells have an efficiency level of 15%-17% and are the most efficient silicon solar cells. Unisilicon and multisilicon cells both comprise silicon semiconductors. However, unisilicon undergoes a pulling process, which causes the silicon to be aligned in the same direction. Therefore, although the efficiency of unisilicon cells is greater, the cost is higher. By contrast, multisilicon solar cells have an efficiency level of 10%-14% and are produced by pressing pure silicon into a crystal and then cutting the crystal into multisilicon cells. Thin film solar panel fabrication requires fewer materials, and each mode in the solar panel acts as a fully functioning panel, thereby reducing the cost of mode connection and fixation.

A solar cell consists of a stable current source, bipolar, and resistance. The charging efficiency depends on the insulation, cell material, surroundings, placement, direction faced, and latitude. Fig. 1 illustrates the internal circuit design of a solar panel [6, 11, 12]; the current output  $I_{pv}$  is

$$I_{pv} = I_{sc} - I_{pvo} \left[ \exp \left( \frac{q(V_{pv} + I_{sc}R_s)}{nKT} \right) - 1 \right], \quad (1)$$

where the terms are

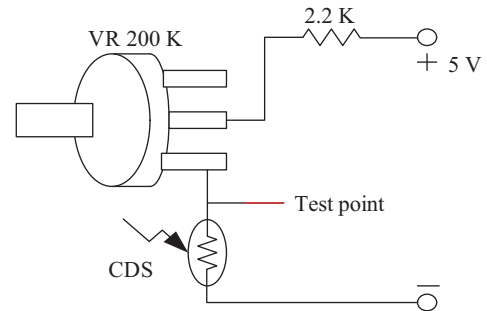


Fig. 2. CdS circuit diagram receiver.

$I_{pv}$	cell output current
$I_{sc}$	electron-hole current from light illumination
$I_{pvo}$	cell saturation current
$q$	electron charge ( $1.602 \times 10^{-19}$ coul)
$V_{pv}$	cell output voltage
$R_s$	series resistance
$n$	ideality factor of solar cell diode
$K$	Boltzmann constant ( $8.63 \times 10^{-5}$ ev/K)
$T$	cell temperature

Methods for monitoring maximal power, including the interference observation method [3, 13, 16] and the increased conduction method [8, 16], have been proposed and are discussed briefly in the following section.

### 2. CdS

A light sensor circuit consisting of light dependent resistors was used in this study to detect the intensity of the sunlight (Fig. 1). The resistance of a light dependent resistor varies according to the amount of light it receives. A protective coating, such as a plated metal film, glass, or resin coating, can be applied to the surface to protect the CdS when used in adverse environments with high temperatures and humidity levels. A weak electric current passes through the CdS even when the CdS is not exposed to sunlight; this is called dark current. Therefore, light dependent resistors have high resistances when they are not subjected to light. Dark current is often treated as noise because its level is much lower than that of light current. A light-dependent resistor is a type of photoelectric sensor based on the internal photoelectric effect. Because of the small size, high sensitivity, stable performance, and low price, light-dependent resistors have been widely applied for automatic control and in many domestic appliances.

Fig. 2 illustrates the CdS circuit diagram used in the present study. The CdS is used to detect the intensity of the sunlight; the value measured is inversely proportional to the intensity of the light source.

### 3. TA7257P Motor Driver IC

1) A TA7257P, a single bridge driver IC (Figs. 3 and 4), is primarily used for controlling single miniature-scaled DC motors. The main characteristics of a TA7257P include [21]

**Table 1. TA7257P Function.**

IN1	IN2	OUT1	OUT2	Mode
1	1	L	L	Brake
0	1	L	H	CW/CCW
1	0	H	L	CCW/CW
0	0			Stop

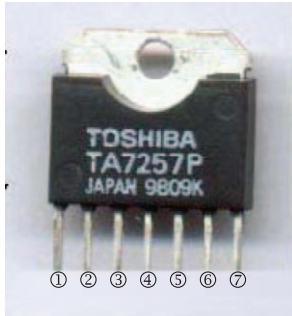


**Fig. 3. TA7257P exterior diagram.**

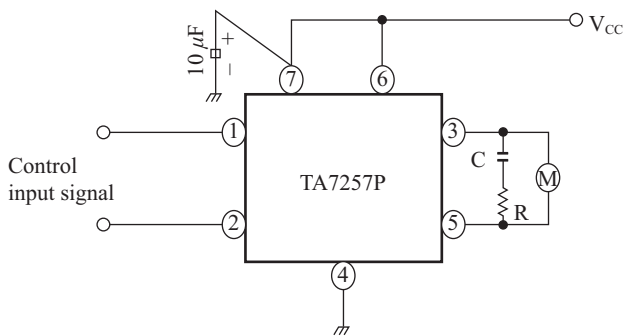


**Fig. 4. TA7257P application circuit diagram.**

forward rotation, reverse rotation, stopping, and fast braking. A logic value of 0 or 1 is held at each leg of the IC. Varying digital combinations of the logic signals are used to achieve the desired control. Table 1 shows these combinations.

- 2) The IC operating voltage and the motor driving voltage are independent. Server control can be used. The operating voltage range for the IC is 6-18 V, and the range of the driving voltage for the motor is 0-8 V (Table 2).
- 3) The IC provides overcurrent protection and a thermal shut-down circuit.
- 4) The IC has an average output current of 1.5 A and a maximal value of 4.5 A.

**4. PCI-DAQ6024E Data Acquisition Card [14]**

Various types of interfaces, including PCI, USB, PCI-E, and PXI, can be used, depending on the specifications of the data acquisition card. We used an A/D card (PCI 6024E) obtained from National Instruments. The properties of this A/D card are as follows: 12 bits, 200 KS/s, 16 analogue inputs, and

**Table 2. PIN function.**

PIN No.	Symbol	Functional description
1	IN1	Input terminal
2	IN1	Input terminal
3	OUT1	Output terminal
4	GND	GND terminal
5	OUT1	Output terminal
6	V <sub>S</sub>	Supply voltage terminal for motor drive (0~8V)
7	V <sub>CC</sub>	Supply voltage terminal for logic (6~18V)

an input signal with a static range between +10 V and -10 V. The resolution of the A/D card was  $20/212 = 4.8828$  mV, because the bipolar input was used. The theoretical signal-to-noise ratio was approximately 74 dB [15]. The preferred single-ended mode supplied by the NI-DAQ PCI 6024E was used as the signal input mode.

**III. SYSTEM SOFTWARE PLANNING**

**1. Introduction of the Human-Machine Interface**

The proposed system was designed using the graphical programming software, LabVIEW; the instrumentation hardware and DAQ-6024E card were connected to the computer. LabVIEW features a comprehensive range of functions for computation, data acquisition, and interface control, and can call dynamic executable files directly. A function in LabVIEW is shown as an ICON. The ICON contains connection points for input-output arguments. LabVIEW does not require a compiler. When a program is written, the ICONs are selected and then arranged according to the required operation. The program can be executed upon connection. Therefore, coding in LabVIEW is simple, even for users who are new to the system [2]. LabVIEW features include powerful control, data extraction, and display functions for curve visualization in real-time. The main tasks for LabVIEW in this study included reading data, processing the data at the interface, and displaying the recorded data in real-time.

The proposed software system uses the LabVIEW block diagram to complete the design (Fig. 5). The A/D conversion is performed on the intensity of the sunlight and the output current from the solar panel by using the data acquisition card, PCI-DAQ6024E.

The results are transferred to a workstation through the serial port. Two variables are used in the fuzzy program computation for real-time detection in LabVIEW (Fig. 6). When activation of the cleaning motors is deemed unnecessary, LabVIEW is employed for further detection. The sunlight continues to shine on the solar cells, increasing power generation. Fig. 7 depicts the front panel diagram from LabVIEW.

**2. Fuzzy Logic Control Theory**

Fuzzy logic theory is a quantitative instrument that was proposed in 1965 by Zadeh, an American scholar in the field

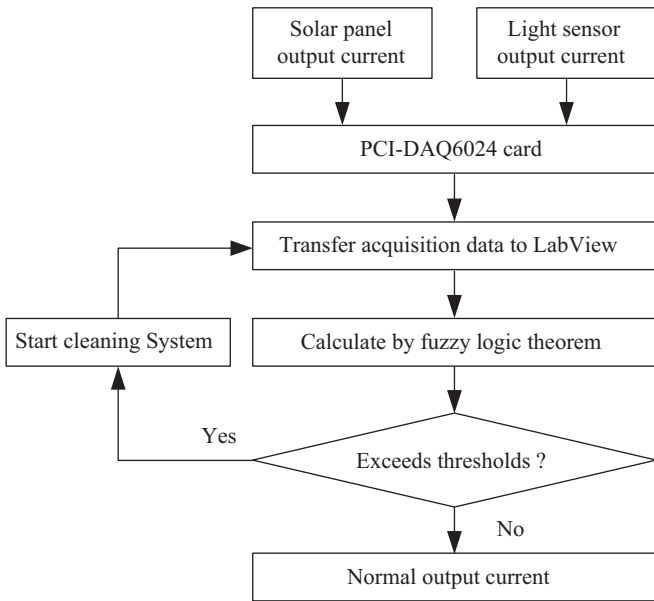


Fig. 5. System software planning flowchart.

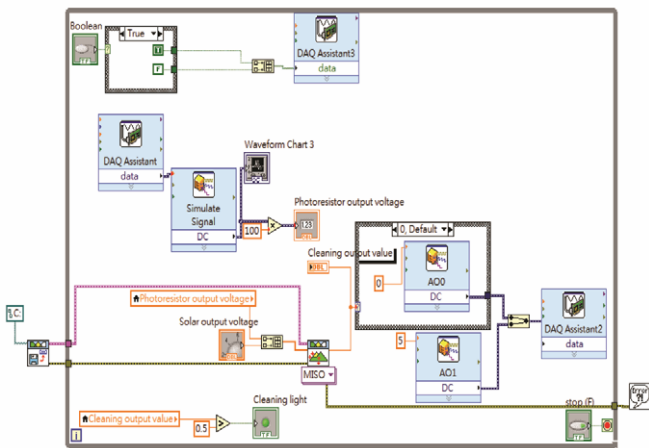


Fig. 6. LabVIEW block diagram.

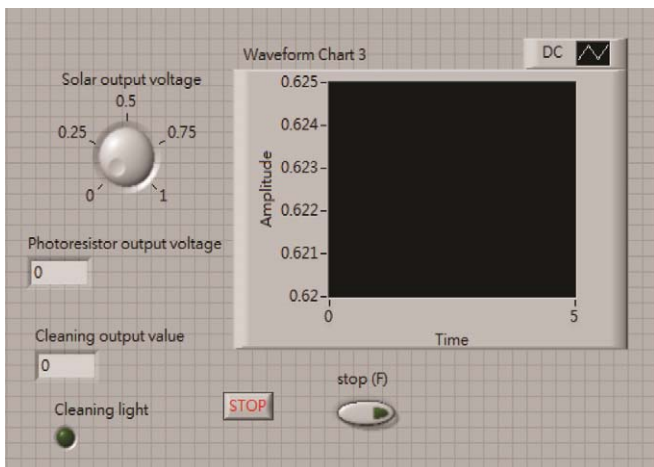


Fig. 7. LabVIEW front panel diagram.

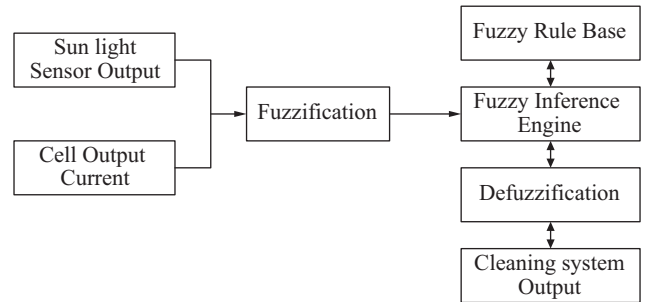


Fig. 8. Flowchart of the fuzzy control theorem.

of control theory. Fuzzy logic theory can be applied to express an ambiguous concept and has worked particularly effectively with the ambiguity of human language. Sugeno, a researcher based in Japan, advocated this theory by researching and developing related applications such as the fuzzy logic controller (FLC), which gained considerable attention [19].

The main advantage of the FLC is that it can be applied in environments in which the controlled body is too complex or difficult for the use of mathematical models. The design of the controller is expressed to ensure that it can reflect a system with few fuzzy rules. In general, fuzzy logic control can be divided into four sections:

- 1) Fuzzification
- 2) Decision-making logic
- 3) Fuzzy knowledge base
- 4) Defuzzification.

In the proposed FLC, the solar panel output current and the sunlight sensor output voltage are used as input values in the fuzzy inference engine (Fig. 5 shows a flowchart for the fuzzy controller). To reduce the number of errors, a membership function is employed, describing the fuzzy set and perform quantitative operations. A continuous trigonometric function is adopted as the membership function:

$$u_{tri}(x) = \left. \begin{array}{ll} 0 & \text{for } x < a_1 \\ \frac{x-a_1}{a_1-a_1} & \text{for } a_1 \leq a \\ 1 & \text{for } x = a \\ \frac{b_1-x}{b_1-a} & \text{for } a < x \leq b_1 \\ 0 & \text{for } x > b_1 \end{array} \right\}. \quad (2)$$

The FLC is applied to the solar panel output current and the sunlight sensor output voltage values. The fuzzy versions of the measured voltages are then used in the fuzzy inference engine as the input values. Fig. 8 shows a flowchart for the fuzzy controller inference engine. Using fuzzy sets and membership functions to quantify the use of triangular membership functions is described in the following.

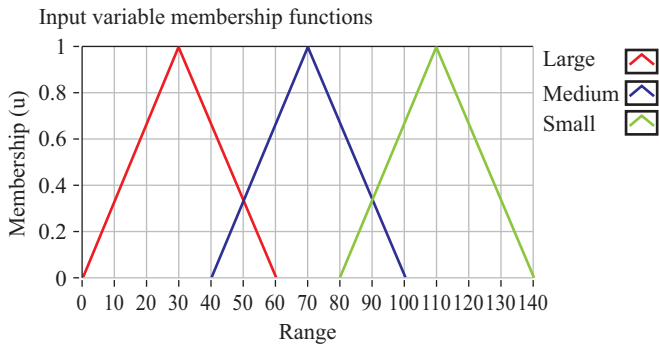


Fig. 9. Membership function of sunlight.

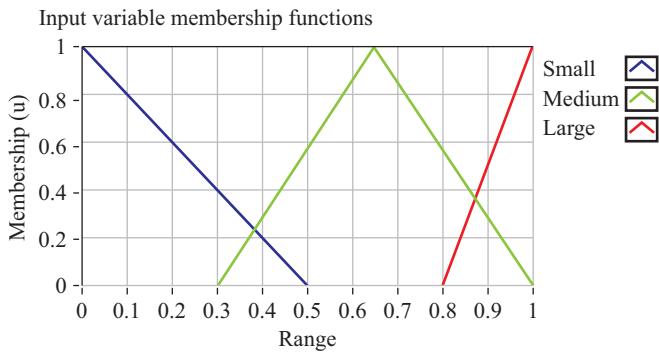


Fig. 10. Membership function of output current.

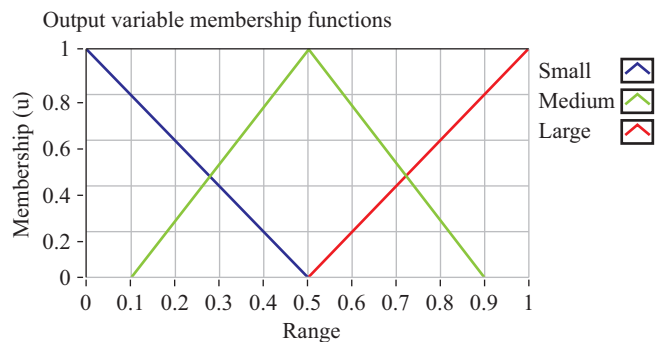


Fig. 11. Membership function of fuzzy output.

The membership functions for the input-output sections of the system are illustrated in Figs. 9-11. The input to the system is the output current of the solar panel and the output voltage of the photo detector. The output of the fuzzy system is used for rotating the solar panels. The ownership function value of each point is between 0 and 1, corresponding to each input variable value. The horizontal axis for the input variable value is also known as the collection element, the size of which is its degree of ownership. The sunlight intensity, solar panel current, and output value can be divided into three states: high, medium, and low.

The second step in fuzzy controller design is determining the form of the fuzzy rules. These rules refer to the relation-

Table 3. Corresponding table of fuzzy rules.

	Sunlight			
Current		Small	Medium	Large
Small		Small	Medium	Large
Medium		Small	Small	Medium
Large		Small	Small	Small

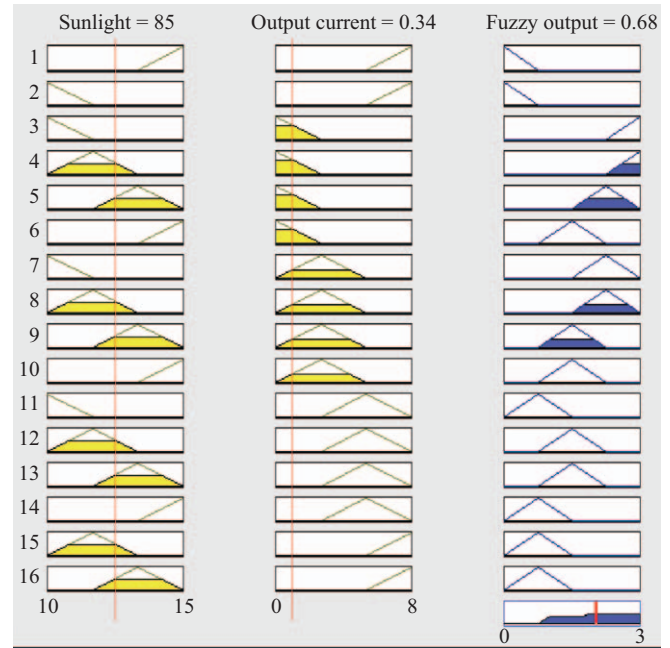


Fig. 12. Fuzzy inference process.

ship between the solar cell output current and the illumination from the sun. The fuzzy rule base shown in Table 3 was obtained using data from the literature.

In the third step of the fuzzy controller design, the type of fuzzy inference engine is selected. We applied the maximum to the Max–Min synthetic fuzzy inference method [15]. The following Max–Min synthetic equation maintains that

$$\frac{\text{if } x_1^\circ \text{ is } X_{11} \text{ and } x_2 \text{ is } X_{21} \text{ than } u \text{ is } U_1}{\text{if } x_2^\circ \text{ is } X_{12} \text{ and } x_2 \text{ is } X_{22} \text{ than } u \text{ is } U_2}, \quad (3)$$

$$u \text{ is } U^0$$

where  $X_{11}, X_{21}, U_1, X_{12}, X_{22}, U_2$  are fuzzy sets;  $x_1^\circ$  and  $x_2^\circ$  are known input variables;  $u$  is the output variable; “than” is “and”; and “and” means taking the intersection (min). Therefore, this system uses combined Max–Min as the fuzzy inference method [7]. According to Fig. 12, the fuzzy output was solved by the defuzzifier. The fitness of the input sections of the fuzzy controller is

$$W_i = \text{Min} \left\{ \max \left[ \min (V_{ai}, V'_a) \right], \max \left[ \min (I_{bi}, I'_b) \right] \right\}, \quad (4)$$

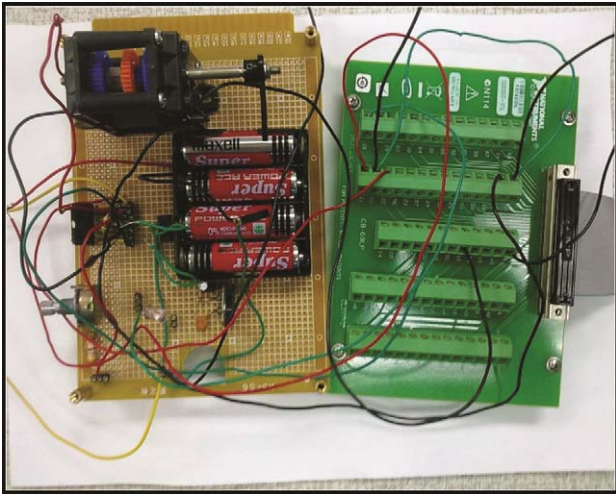


Fig. 13. Photo of hardware used to drive the cleaning motors.

where  $V$  is the sunlight intensity and  $I$  is the current from the solar panels.

The fitness of the output sections is

$$B'_i = \min(W_i \mu_{B_i}(y)), \quad (5)$$

where  $i$  is the rule number,  $V'_a$  and  $I'_b$  are inputs, and  $\mu$  is the output.

All rules are set as

$$B = \underset{i=1}{\overset{r}{\text{Max}}} B'_i. \quad (6)$$

where  $r$  is the number of triggered rules.

Eqs. (4)-(6) express the fuzzy controller process. In this study, we used the LabVIEW Fuzzy Logic Toolbox to determine the fuzzy controller output value. We then determined the output value according to this chart. We set the threshold level of the fuzzy output value at 0.5. A value of 0.5 or greater activated the cleaning system.

#### IV. NUMERICAL SIMULATION AND ANALYSIS

Fig. 13 shows the hardware driving system, which consists of hardware connected to an NI-DAQ PCI 6024E data acquisition card that is linked to a workstation. The CdS and the output current from the solar panel data values are collected. A/D conversion is performed using a DAQ data acquisition card. The LabVIEW graphical programming language receives the input values, including the intensity of the light source and the current from the solar panel, and involves applying fuzzy logic to determine the output, which is used to determine whether cleaning is required. When the output value exceeds or is equal to 0.5, A/D conversion is performed

Table 4. Comparison chart of the fuzzy theory.

Fuzzy output value	Intensity of the sunlight (V)					
	0.25	0.45	0.65	0.85	1.05	1.45
Output current from solar panel (A)						
0.1	0.8276	0.6665	0.5001	0.4625	0.1724	0
0.2	0.8131	0.6611	0.5002	0.4666	0.1874	0
0.3	0.7739	0.6423	0.4968	0.4554	0.2056	0
0.4	0.5457	0.5003	0.3826	0.3826	0.2148	0
0.5	0.5002	0.4629	0.1873	0.1972	0.1873	0
0.6	0.5002	0.4668	0.1694	0.1964	0.1694	0
0.7	0.5001	0.4689	0.1705	0.1972	0.1705	0
0.8	0.4931	0.4629	0.1898	0.1964	0.1898	0
0.9	0.3524	0.3653	0.1941	0.1972	0.1941	0
1.0	0.1699	0.1963	0.1692	0.1972	0.1692	0

by the DAQ data acquisition card, and the signal is sent to the TA7257P motor driver IC to drive the motor and perform the cleaning operation.

We verified the accuracy of the software planning after we evaluated the process of the hardware structure driving system. The CdS value measured under sunlight was 0.25 V. The output current from the solar panel was 0.1 A, and the test output value from the fuzzy program was 0.82756; thus, the motor was activated for cleaning. When we performed the experiment again, but placed the device in the shade, the CdS value was 0.7 V. The output current from the solar panel was 0.2 A, and the test output value from the fuzzy program was 0.5002, again exceeding the threshold of 0.5. Therefore, the motor was activated to perform cleaning. Finally, when the device was entirely covered, the CdS value was 0.125 V. The output current from the solar panel was 0.5 A, and the test output value from the fuzzy program was 0.1873 (i.e., below the threshold). In this case, the motor was not activated for cleaning. The results from the fuzzy program are accurate (Table 4).

#### V. CONCLUSION

The proposed solar panel cleaning system is based on fuzzy logic control. According to our research, no solar panels currently on the market are equipped with cleaning devices. Over time and with varying weather conditions, deposits can accumulate on installed solar panels, producing shadows on the solar cells and causing the conversion efficiency to drop. In addition, some dust particles are corrosive, reducing the life span of the solar cells and their supporting frames. We developed a device for panel cleaning, which improves the output current of the solar panels.

The solar panel cleaning system based on fuzzy logic control uses the output current from single-axis tracker solar cells to calculate the fuzzy output. In the future, we anticipate using solar cells with dual-axis trackers with this system. The temperature of solar cells in direct sunlight can be extremely high. Thus, future studies can investigate the effect of temperature on the conversion efficiency. In addition to the cleaning process, a water spraying system can be applied to lower the temperature; this will afford a comprehensive system that ensures maximal conversion efficiency of the solar cells.

### ACKNOWLEDGMENTS

The author would like to thank the National Science Council of the Executive Yuan, Taiwan, R.O.C., for financially supporting this study under contract NSC 102-2221-E-269-018.

### REFERENCES

1. Bull, S. R., "Renewable energy today and tomorrow," *Proceedings of the IEEE*, Vol. 89, No. 8, pp. 1216-1226 (2001).
2. Chouder, A., Silvestre, S., Taghezouit, B., and Karatepe, E., "Monitoring, modelling and simulation of PV systems using LabVIEW," *Solar Energy*, Vol. 91, No. 5, pp. 337-349 (2013).
3. Fraidenraich, N. and Vilela, O. C., "Dynamic behavior of water wells coupled to PV pumping systems," *Progress in Photovoltaics: Research and Applications*, Vol. 15, No. 4, pp. 317-330 (2007).
4. Gao, L. J. and Dougal, R. A., "Parallel-connected solar PV system to address partial and rapidly fluctuating shadow conditions," *IEEE Transactions on Industrial Electronics*, Vol. 56, No. 5, pp. 1548-1556 (2009).
5. Gules, R., Pacheco, J. D. P., Hey, H. L., and Imhoff, J., "A maximum power point tracking system with parallel connection for PV stand-alone applications," *IEEE Transactions on Industrial Electronics*, Vol. 55, No. 7, pp. 2674-2683 (2008).
6. Hoen, B., Wiser, R., Thayer, M., and Cappers, P., "Residential photovoltaic energy systems in California: the effect on home sales prices," *Contemporary Economic Policy*, Vol. 31, No. 4, pp. 708-718 (2013).
7. Hsieh, G. C., Chen, L. R., and Huang, K. S., "Fuzzy-controlled Li-Ion battery charge system with active state-of-charge controller," *IEEE Transaction on Industrial Electronics*, Vol. 48, No. 3, pp. 585-593 (2001).
8. Hussein, K. H., Muta, I., Hoshino, T., and Osakada, M., "Maximum photovoltaic power tracking: an algorithm for rapidly changing atmospheric conditions," *IEE proceeding on Generation Transmission Distribution*, Vol. 142, No. 1, pp. 59-64 (1995).
9. Lee, S. C., "Numerical estimation model of energy conversion for small hybrid solar-wind system," *Solar Energy*, Vol. 86, No. 11, pp. 3125-3136 (2012).
10. Liu, Y. H., Liu, C. L., Huang, J. W., and Chen, J. H., "Neural-network-based maximum power point tracking methods for photovoltaic systems operating under fast changing environments," *Solar Energy*, Vol. 89, No. 3, pp. 42-53 (2013).
11. Markvart, T., *Solar Electricity*, John Willy & Sons (1995).
12. Nakanishi, F., Ikegami, T., Ebihara, K., Kuriyama, S., and Shiota, Y., "Modeling and operation of a 10 kw photovoltaic power generator using equivalent electric circuit method," *Photovoltaic Specialists Conference*, pp. 1703-1706 (2000).
13. Oman, H., "Battery developments that will make electric vehicles tactical," *IEEE Aerospace & Electronics Systems Magazine*, Vol. 1, No. 8, pp. 11-21 (2000).
14. Potter, D., *DAQ 6023E/6024E/6025E User Manual*, National Instruments Corporation (2000).
15. Potter, D., *Using Ethernet for Industrial I/O and Data Acquisition*, National Instrument Corporation (2000).
16. Pradhan, A., Ali, D. S. M., Jena, C., and Behera, P., "Design and simulation of DC-DC converter used in solar charge controllers," *International Journal of Engineering Inventions*, Vol. 2, No. 3, pp. 59-62 (2013).
17. Rahman, S., "Green power: what is it and where can we find it?" *IEEE Power and Energy Magazine*, Vol. 1, No. 1, pp. 30-37 (2003).
18. Razykov, T. M., Ferekides, C. S., Morel, D., Stefanakos, E., Ullal, H. S., and Upadhyaya, H. M., "Solar photovoltaic electricity: current status and future prospects," *Solar Energy*, Vol. 85, No. 8, pp. 1579-1726 (2011).
19. Seising, R., "40 years ago: 'fuzzy sets' is going to be published," *IEEE International Conference on Fuzzy Systems*, Vol. 3, pp. 1589-1594 (2004).
20. Stern, M. J. and West, R. T., "Development of a low cost integrated 15 kw A.C. solar tracking subarray for grid connected PV power system applications," *Proceedings of AIP Conference*, Vol. 394, pp. 827-833, Lakewood, Colorado, USA (1996).
21. TOSHIBA, Toshiba Bipolar Linear Integrated Circuit Silicon Monolithic TA7257P, Datasheets for electronics components (2001).